Food and Chemical Toxicology 206 (2025) 115738

Contents lists available at ScienceDirect

Food and Chemical Toxicology

journal homepage: www.elsevier.com/locate/foodchemtox

# Subacute exposure of 2, 2′, 4, 4′-tetrabromodiphenyl ether induced liver injury by inhibiting mitochondrial autophagy and increasing NLRP3 inflammasome in mice

Xiyue Cao [b,c], Weijue Liu [b], Shuhua Xi [b], Yue Wang [a,b,*]

[a] School of Public Health, Shenyang Medical College, No. 146 Huanghe North Street, Shenyang, 110034, China
[b] Department of Environmental Health, School of Public Health, China Medical University, Shenbei New District, Puhe Road, No.77, Shenyang, Liaoning Province, 110122, China
[c] Disease Prevention and Control Center of Jinpu District, 71-1 Liaohe West Road, Maqiaozi Street, Dalian, Liaoning Province, 116000, China

ARTICLE INFO

Handling Editor: Professor Matthew Wright

*Keywords:*
BDE-47
Liver damage
Mitophagy
NLRP3 inflammasome

ABSTRACT

2′,4,4′-tetrabrominated diphenyl ethers (BDE-47) is one of the most common brominated flame retardants found in environment and has been demonstrated to be associated with a variety of adverse human health effects. It has been proven to generate liver toxicity, but little is known about the potential mechanism following BDE-47 exposure. Here, hepatotoxicity of BDE-47 in mice was investigated by gavage exposure to BDE-47 (12.5–100mg/kg/day) for 4 weeks. The results showed the increasing of ALT and AST in serum and histopathological change of liver in BDE-47 exposure mice. In addition, we observed that the mitochondrial membrane potential (MMP) decreased and ROS increased with the increase of BDE-47 dose. BDE-47 also up-regulated NLRP3 protein levels, and proteins expression of caspase-1, IL-1β, IL-18 and TNF-α inflammatory factors. Furthermore, mitophagy was blocked with Parkin and PINK1 protein expression decrease and P62 increase in liver of BDE-47 exposure mice. However, activation of mitophagy with autophagy activator rapamycin (RAPA) alleviated liver injury induced by BDE-47 in mice via increasing the protein expression of PINK1 and Parkin, and decreasing NLRP3 and inflammatory factors. These results suggest NLRP3 inflammasome activation-mediated mitochondrial and liver damage in BDE-47-exposed mice is due to mitophagy downregulation, and activating mitophagy can alleviate BDE-47-induced inflammatory damage by regulating NLRP3 inflammasome.

## 1. Introduction

Polybrominated diphenyl ethers (PBDEs) are frequent brominated flame retardant used widely in electronic devices, furniture, textiles, building materials for many years. The concentrations of PBDEs in the environment have been increasing. PBDEs are of great concern due to their potential toxicity, durability and bioaccumulation. PBDEs are toxic to the liver, nervous system, endocrine system and immune system, and can induce cancer. Although the use of brominated flame retardants has been banned at present, a large amount of brominated flame retardants still exists in the soil, water and organisms and posing a significant threat to humans. Air samples collected during the four seasons of 2009 at a sampling site in Beijing showed that the concentrations of PBDEs ranged from 57 to 470 pg/m$^3$(Hu et al., 2011). Testing results from 3971 food samples provided by the European Food Safety Authority indicated that the median dietary exposure to 2′,4,4′-tetrabrominated diphenyl ethers (BDE-47) was 1.8 ng/kg bw(Fromme et al., 2016). In North American populations, the concentration of 6-PBDEs in blood was measured at 9.5–21.1 1.8 ng/kg lw(Foster et al., 2011). Among these, BDE-47 accounted for the highest proportion, approximately 57 %, of the total 6-PBDE congeners(Foster et al., 2011). BDE-47 is one of the most commonly detected PBDEs in environmental and biological samples, characterized by its toxicity, lipophilicity, bioaccumulation, and resistance to degradation. BDE-47 is mainly ingested and inhaled into the human body and can be detected in various human samples including blood, fat tissue and breast milk. Due to its lipophilicity and long half-life, BDE-47 prone to accumulate in lipid-rich tissues such as fat and liver. The liver, acting as the key organ for human digestion and detoxification, is the main target organ for BDE-47 toxicity. Several studies have revealed that hepatic oxidative stress, abnormal fatty acid oxidation, DNA damage and apoptosis following exposure to BDE-47

* Corresponding author. School of Public Health, Shenyang Medical College, No. 146 Huanghe North Street, Shenyang, 110034, China.
*E-mail address:* yuewang@cmu.edu.cn (Y. Wang).

https://doi.org/10.1016/j.fct.2025.115738
Received 23 April 2025; Received in revised form 6 September 2025; Accepted 10 September 2025
Available online 11 September 2025

**Abbreviations**

| | |
|---|---|
| ALT | Alanine transaminase |
| AST | Aspartate transaminase |
| BDE-47 | 2′,4,4′-tetrabrominated diphenyl ethers |
| LC3 | Microtubule-associated proteins 1A/1B light chain 3 |
| IL-1β | Interleukin-1 β |
| IL-18 | Interleukin-18 |
| Caspase-1 | Cysteinyl aspartate specific protease |
| MMP | Mitochondrial membrane potential |
| NLRP3 | NOD-like receptors containing pyrin domain 3 |
| Parkin | Parkinson disease2 |
| PBDEs | Polybrominated diphenyl ethers |
| PINK1 | PTEN-induced putative kinase 1 |
| RAPA | Rapamycin |
| ROS | Reactive oxygen species |
| TEM | Transmission electron microscope |
| TNF-α | Tumor necrosis factor –α |

(Meng et al., 2020; Wang et al., 2022). Moreover, BDE-47 exposure induced liver injury through liver inflammatory response (Zhang et al., 2015a). It was reported that the NOD-like receptors containing pyrin domain 3 (NLRP3) inflammasome signaling pathway was activated in hearing damage induced by BDE -47 (Tang et al., 2021). Inflammasome is a multi-protein complex that is assembled with cytoplasmic pattern recognition receptor (PRRs) and is an important component of the innate immune system. Among many inflammasomes, NLRP3 inflammasome plays important roles in the immune system and inflammatory diseases. NLRP3 inflammasome is composed of a receptor protein (NLRP3), an adaptor protein (ASC), and anector protein (pro-caspase-1). The NLRP3 inflammasome is a self-defense mechanism against invading factors and stress when activated. Upon infection or injury, the parts of the inflammasome assemble and oligomerize, leading to auto-cleavage of pro-caspase-1 into its active form. The activated caspase-1 further cleaves the proinflammatory cytokines IL-1β and IL-18 of the IL-1 family. The mechanisms of NLRP3 inflammasome activation include ionic channel, lysosomal damage, increased reactive oxygen species (ROS) and mitochondrial dysfunction (Kelley et al., 2019). BDE-47 impaired mitochondrial bioenergetics by affecting inner membrane, membrane potential, oxygen consumption in rat liver mitochondria (Gomez et al., 2015). BDE-47 led to nephrotoxicity by induced mitochondrial dysfunction and triggered NLRP3 inflammasome and GSDMD-dependent pyroptosis in renal tubular epithelial cells in vitro (Zhang et al., 2022).

Mitochondria are key organelles involved in aerobic respiration, metabolic processes, energy production, and the first line of defense for cells under various stress conditions. When mitochondria is damaged, cells will initiate mitophagy for maintaining mitochondrial homeostasis and enhancing cellular self-defense capacity (Chen et al., 2020). In mammals, multiple signaling pathways are involved in mitophagy, among which the PTEN-induced putative kinase 1 (PINK1)/Parkinson disease 2 (Parkin) signaling pathway-mediated mitophagy is currently the most classical mitophagy pathway. PINK1 is a serine/threonine kinase and locates on outer mitochondrial membrane. Parkin is an E3 ubiquitin ligase that mediates substrate ubiquitination, modulates protein degradation, and regulates environmental balance within mitochondria in specific stress practices (Pickrell and Youle, 2015). PINK1 recruits Parkin to mitochondria by phosphorylating Parkin and ubiquitin to activate its E3 ligase during stress, which leads to the activation of the Parkin E3 ligase and the ubiquitination of outer mitochondrial membrane proteins, ultimately clearing the damaged mitochondria by mitophagy (Han et al., 2020). Mitophagy can specifically clear damaged mitochondria and plays an important role in guaranteeing mitochondrial quality and quantity (Doblado et al., 2021). In recent years, studies have shown that mitophagy might be involved in inhibiting the activation of NLRP3 inflammasome. PINK1/parkin pathway of mitophagy inhibited NLRP3 inflammasome activation and reduced contrast-induced acute kidney injury (Lin et al., 2019). Mitophagy could protect mice from paracetamol-induced acute liver injury by inhibiting the activation of the NLRP3 inflammasome (Shan et al., 2019). Impaired mitophagy results in decreased clearance of damaged mitochondria, which leads to cell lethal changes. BDE-47 could disrupt mitochondrial homeostasis because of impaired mitophagy, then triggering apoptosis, and subsequent neurobehavioral deficits (Dong et al., 2023). Our previous studies found that BDE-47 impaired placental angiogenesis by increasing apoptosis and autophagy in mice (Liu et al., 2022). However, it is unknown whether mitophagy can regulate NLRP3 inflammasome activation in BDE-47-induced liver injury in mice.

Here, we investigated the relationship between NLRP3 inflammasome and mitophagy in liver injury by establishing a mouse model with BDE-47 exposure and autophagy activator (rapamycin) intervention. The results will provide basic research data for the prevention and control of BDE-47 pollution.

## 2. Materials and methods

### 2.1. Animals and treatment

The SPF-grade male 6–8-week-old ICR mice were purchased from Liaoning Chang sheng Biological Co., Ltd. (Liaoning, China). The mice were subjected to temperature at 20 ± 2 °C, humidity at 55 % ± 10 %, and light in light-dark cycle, free drinking and feeding. The mice were adaptive fed for a week before the experiment began. In experiment one, 40 mice were randomly divided into 5 groups with 8 mice in each group. BDE-47 was dissolved in corn oil and mice were given 0, 12.5, 25, 50 and 100 mg/kg/day BDE-47 by gavage every morning for 4 weeks. The exposure doses of BDE-47 come from our research group's previous work (Liu et al., 2022). After exposure for 4 weeks, the mice were anesthetized with a 20 % urethane solution (1 ml/100 g body weight) intraperitoneally, and blood was taken and centrifugated immediately. The supernatant was stored at a low temperature to detect the related indexes. 1 mm long, 1 mm wide and 2 mm high of fresh liver tissue of mouse (four mice in each group) was fixed with 2.5 % malondialdehyde for electron microscope. The residual liver tissues were removed and stored as spare parts in a −80 °C refrigerator. In experiment two, 32 mice were randomly divided into control group, 5 mg/kg/day rapamycin (RAPA) group, 50 mg/kg/day BDE-47 group, and 5 mg/kg/day RAPA + 50 mg/kg/day BDE-47 group with 8 mice in each group. The mice were intraperitoneally injected with saline for the control group and BDE-47 group, and RAPA for RAPA group and RAPA + BDE-47 group 1 h before oral administration with corn oil (the control group and RAPA group) or BDE-47 (BDE-47 group and RAPA + BDE-47 group). After 4 weeks of exposure, the mice were anesthetized by intraperitoneal injection of 20 % urethane solution (1 ml/100 g body weight), and the experimental operation was the same as the experiment one. This study adhered to the ethical guidelines set forth in the Guide for the Care and Use of Laboratory Animals endorsed by the National Institutes of Health. Animal experiments complied with the UK Animals (Scientific Procedures) Act, 1986 and associated guidelines, and EU Directive 2010/63/EU for animal experiments. All animal procedures were approved by the Laboratory Animal Welfare and Ethical Committee of China Medical University (approval number CMU202102050).

### 2.2. Alanine transaminase (ALT) and aspartate transaminase (AST) assay in mice serum

Samples were prepared by diluting serum supernatants in a certain proportion and determined according to the instructions of ALT Assay Kit (#C009-2-1) and AST Assay Kit (#C010-2-1). The activities of ALT

and AST were determined by microplate method. The absorbance value of the diluted serum was determined at 510 nm with an enzyme labeled instrument. The contents of ALT and AST were calculated according to the instruction manual. All assay kits were obtained from Jiancheng Biotechnology Co. Ltd (Nanjing, China).

### 2.3. Hematoxylin and eosin (H&E) staining

Freshly collected liver tissues were fixed in 4 % paraformaldehyde for 24 h, then dehydrated with an alcohol gradient, soaked in xylene to make it transparent, and embedded in paraffin. Paraffincontaining liver tissue was sectioned at 5 μm. After deparaffinization, sections were stained with hematoxylin and eosin (H&E) and then scanned using a highresolution total-mirror imaging system (CS2, Leica, Germany).

### 2.4. Immunofluorescence in mice liver

The liver samples were fixed in 4 % paraformaldehyde, embedded in paraffin and cut into thin sections. The sections of liver tissue were dewaxed with xylene and dehydrated with gradient alcohol to depolarize them. After paraffin removal, the sections were blocked with BSA blocking solution at 37° for 30 min, and then incubated with primary antibodies (NLRP3, #A5652 ABclonal Technology, Wuhan, China) overnight at 4 °C. Then the sections were incubated with fluorescent secondary antibodies at room temperature for 2 h in the dark. The nuclei were stained with DAPI. After wrapping with a fluorescence quenching agent, the sections were photographed using an inverted fluorescencemicroscope (Leica, Germany) and fluorescence density was analyzed with ImageJ software.

### 2.5. Western blot

Liver tissue was lysed in precooled RIPA buffer (containing phosphatase inhibitor and protease inhibitor) using a tissue homogenizer, and the supernatant was extracted by centrifugation. BCA protein concentration assay kit (BCA03, DingGuo changSheng Biotech. Co. Ltd, Beijing, China) was used to quantify protein concentration. Western Blot was performed according to previous method (Liu et al., 2022). The antibodies were as follows: NLRP3 Rabbit pAb (#A5652, ABclonal, China), Interleukin-β (IL-1β) Rabbit pAb (#A16288, ABclonal, China), Interleukin-18 (IL-18) Rabbit pAb (#A1115, ABclonal, China), cysteinyl aspartate specific protease-1 (Caspase-1) Rabbit pAb (#A16792, ABclonal, China), Tumor necrosis factor-α (TNF-α) Rabbit pAb (#A0277, ABclonal, China), PINK1 Rabbit pAb (#A11435, ABclonal, China), Parkin Rabbit pAb (#A11172, ABclonal, China), Microtubule-associated proteins 1A/1B light chain 3 (LC3) Rabbit pAb (#4108, Cell Signaling Technology, America), P62 Rabbit pAb (#A21440, ABclonal, China), GAPDH Rabbit pAb (#A2118, Cell Signaling Technology, America).

### 2.6. Mitochondrial membrane potential

The single-cell suspension was prepared as follows: 50 mg of liver each mouse was washed twice with PBS and cut with scissors, and then digested with 2 ml 0.25 % trypsin in 37 °C water bath for 10min. The suspension was filtered through 100 mesh and 200 mesh sieves respectively and transferred to a 1.5 ml EP tube, after centrifugation at 1000 rpm for 10 min at room temperature, the supernatant was aspirated and the cells were resuspended in 500 μl culture medium. 500 μl JC-1 (#C2006, Beyotime, China) staining solution was added to the single-cell suspension in each tube, which was mixed and shaken in a 37 °C incubator. After 20 min in the dark, the single-cell suspension was centrifuged at 600 g, 4 °C for 3min, and the supernatant was discarded, the remaining cells were resuspended in a flow tube with appropriate amount of 500 μl PBS staining, and the mitochondrial membrane potential (MMP) was detected with FASC CantoII Flow cytometry.

### 2.7. Reactive oxygen species (ROS) assay

The single-cell suspension was prepared as the same as mitochondrial membrane potential. 500 μl MitoSOX Red (#S0033s, Beyotime, China) was added to the single-cell suspension, and the supernatant was put into a 37 °C incubator after mixing and shaking. After 20 min in the dark, the single-cell suspension was centrifuged at 600 g, 4 °C for 3min, and the supernatant was discarded, the remaining cells were resuspended with 500 μl PBS and ROS was measured with FASC CantoII Flow cytometry.

### 2.8. Transmission electron microscopy

After the mice were executed, the livers were quickly harvested and grown into tissue blocks of 1 mm in length, 1 mm in width and 2 mm in height, which were immersed in 2.5 % glutaraldehyde and stored in a 4 °C refrigerator for 2 h. After washing with buffer for three times, liver tissue blocks were fixed in 10 g/L osmium tetroxide at 4 °C for 90 min, and washed three times with distilled water. The samples were dehydrated in 30 %, 50 %, 70 %, 8 %, 90 %, and 100 % alcohol for 5 min each, twice. Then the samples were put into 100 % propylene oxide for 5 min, twice, and in the resin to propylene oxide at a ratio of 1: 1 for 1 h, pure resin infiltration for 1 h. Subsequently, embedding is performed and then polymerization in the embedding plate at 45 °C for 12 h and60 °C for 24 h. Ultra-thin sections of 50 nm were cut with an ultramicrotome and placed on copper grids. The sections were treated with 20 g/L uranyl acetate and 26 g/L lead citrate, dried overnight, and then observed under a JEM-1400 Flash transmission electron microscope (Japan Electronics).

### 2.9. Statistical analysis

All data were analyzed using SPSS version 23.0 software (SPSS Inc., Chicago, IL, USA), and tested for normality using the Shapiro–Wilk test before further statistical analysis. The results of normality tests are shown in Table S1–2. Differences among groups were compared using one-way analysis of variance (ANOVA) or min to max, and differences between groups were performed using SNK test and Dunnett's T3 test for ALT, AST, inflammatory factors protein expressions. Statistical plotting was performed using GraphPad Prism 8.0 software. Data were presented as mean ± standard deviation (SD) or min to max, and statistically significant differences were considered as $P < 0.05$.

## 3. Results

### 3.1. BDE-47 exposure induced liver injury in mice

During the whole exposure process, the all mice showed smooth of fur, behaved normally, and there was no obvious abnormality. There was no significant differences among groups for body weight ($P > 0.05$) (Fig. 1A). ALT and AST are elevated in most chronic and acute liver diseases, and are markers for liver injury. In this study, the activities of ALT and AST in serum of mice increased with the dose of BDE-47. There were significant differences at 25 mg/kg/day, 50 mg/kg/day and 100 mg/kg/day BDE-47 groups as compared with the control group for ALT and AST levels ($P < 0.01$) (Fig. 1B). Then, we examined the pathological changes in the liver. H&E staining showed that the intercellular space of hepatocytes in BDE-47 groups was larger than that in the control group, as shown in Fig. 1C. In addition, cell swelling was obvious in 50 mg/kg/day and 100 mg/kg/day BDE-47 group. These results indicated that BDE-47 exposure induced liver injury in mice.

### 3.2. Effects of BDE-47 exposure on liver mitochondria in mice

To determine the effect of BDE-47 exposure on liver mitochondria in mice, we observed the morphological changes of mitochondria under

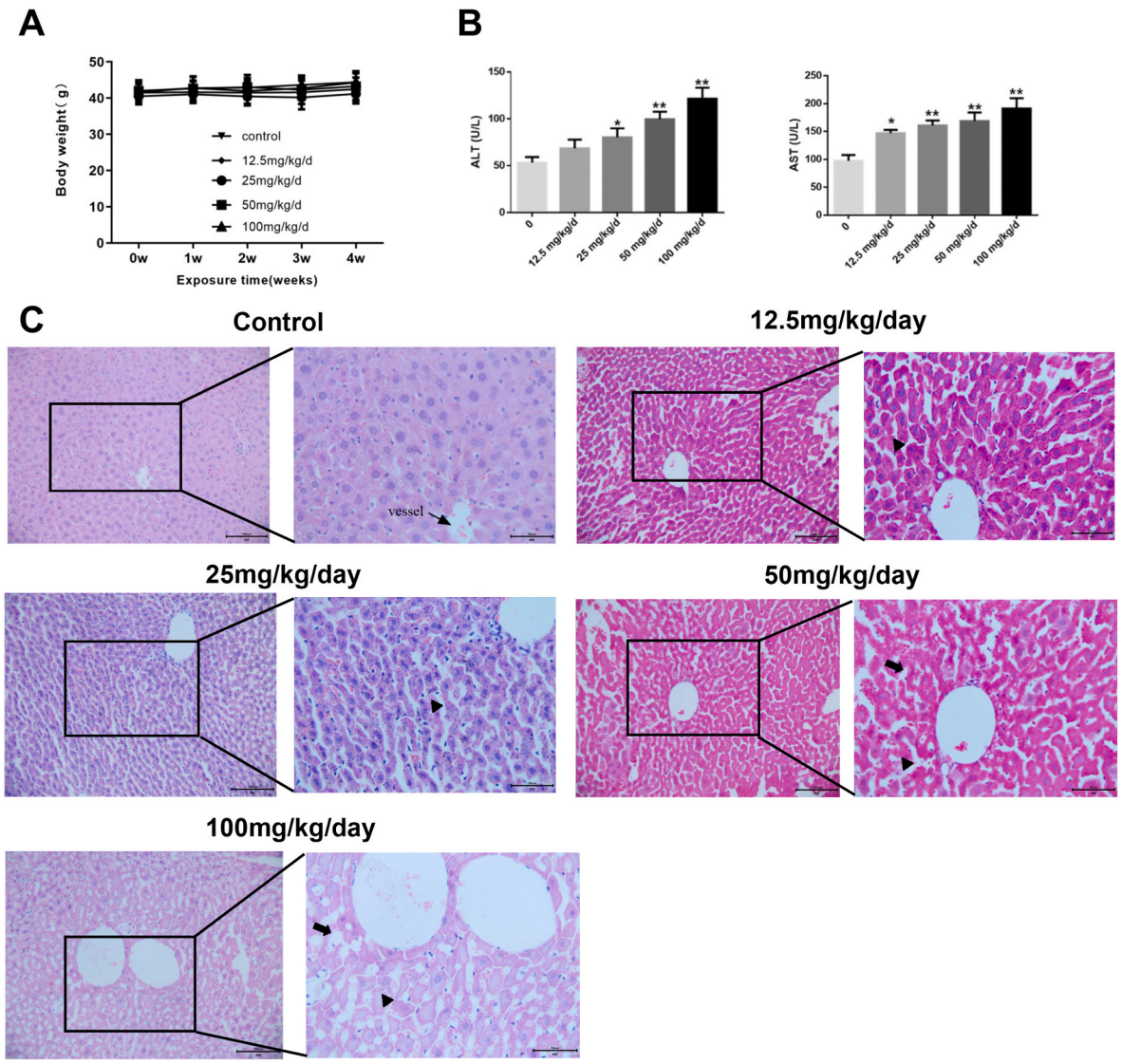


**Fig. 1.** BDE-47 exposure induces liver injury in mice. A Body weight of mice, n = 8; B ALT and AST levels in serum of mice, n = 6; C Representative images of H&E staining to observe liver damage. Magnification: 20× and 40 × , Bar = 100 μm and 50 μm. Black triangle: enlarged spaces; Black thick arrowhead: cell swelling. Data are expressed as mean ± SD. *$P < 0.05$ compared to control group and **$P < 0.01$ compared to control group. BDE-47: 2′,4,4′-tetrabrominated diphenyl ethers.

transmission electron microscope (TEM). As shown in Fig. 2A, BDE-47 induced swelling of mitochondria matrix, breakage of mitochondrial membrane, irregular morphology of mitochondria, and disappearance of mitochondrial cristae structure. In addition, the damage of mitochondria was more serious in the 100 mg/kg/day BDE-47 group. The decline of MMP is a key feature of mitochondrial dysfunction. We found that the MMP decreased gradually with the increase of BDE-47 dose by the Flow cytometry, and there was a significant difference between the 50 mg/kg/day or 100 mg/kg/day dose groups and the control group ($P < 0.05$), see Fig. 2B. Furthermore, we found that ROS levels in the liver of the 50 mg/kg/day and 100 mg/kg/day BDE-47 groups were significantly higher than those of the control ($P < 0.05$), and there was a significant dose-response relationship ($r = 0.751$, $P < 0.01$) (Fig. 2C). ROS is one of the main ways to cause mitochondrial damage. These results suggested that BDE-47 exposure caused damage to liver mitochondria in mice.

### 3.3. BDE-47 activated the NLRP3 inflammasome and promoted the expression of its downstream inflammatory factors

To determine the inflammation of liver tissues induced by BDE-47, the activation of the NLRP3 inflammasome and its downstream inflammatory factor protein expression were determined. It was found that the protein expression of NLRP3 increased with the dose of BDE-47 exposure (Fig. 3A and B). NLRP3 protein levels were significantly increased in BDE-47 exposure groups at 25 mg/kg/day, 50 mg/kg/day and 100 mg/kg/day compared with the control group ($P < 0.01$). The protein expression of inflammatory factors such as TNF-α, IL-1β, Caspase-1 and IL-18 in liver tissues also increased after exposure to BDE-47 (Fig. 4A). The protein expression levels of IL-18 and Caspase-1 in BDE-47 exposure groups at 50 mg/kg/day and 100 mg/kg/day were higher than those in the control group ($P < 0.05$ or $P < 0.01$), and IL-1β and TNF-α protein expressions in 25 mg/kg/day, 50 mg/kg/day and 100 mg/kg/day BDE-47 exposure groups were higher than the control group ($P < 0.05$ or $P < 0.01$). These results suggested that BDE-47 exposure could activate NLRP3 inflammasome in mouse liver and induce cellular inflammatory response.

### 3.4. Effects of BDE-47 on mitophagy in mouse liver

When mitochondria are damaged, cells initiate mitophagy to clear damaged mitochondria and ensure the normal structure and function of

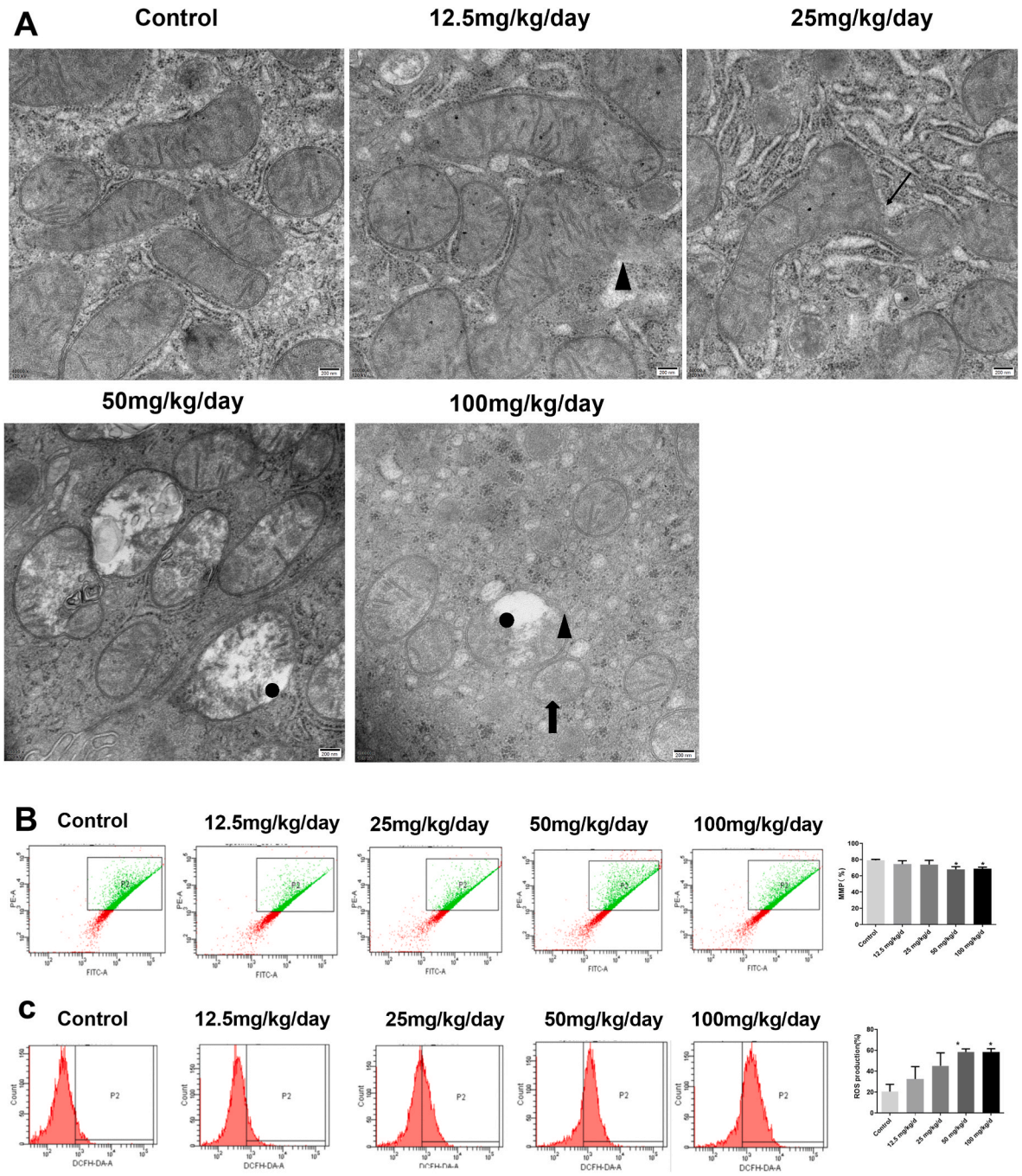


**Fig. 2.** Effects of BDE-47 exposure on liver mitochondria in mice. A Mitochondrial morphology was evaluated by TEM. Black thin arrow indicates irregular morphology of mitochondria: Black thick arrow indicates disappearance of mitochondrial cristae structure: Triangle indicates breakage of mitochondrial membrane; Circle indicates mitochondria matrix swelling. Magnification: 40000×, Bar-200 nm; B Flow cytometry detection of MMP in mouse liver; C ROS levels in liver of mice by Flow cytometry. Data are expressed as mean ± SD. n = 3 * P < 0.05 compared to control group. BDE-47: 2′,4,4′-tetrabrominated diphenyl ethers.

cells. Previously, we found that BDE-47 exposure damaged mitochondria and decreased MMP of liver. Therefore, the expression of mitophagy-related proteins was further examined. As shown in Fig. 4B, Parkin and PINK1 protein expression levels decreased significantly with increasing BDE-47 exposure doses, and there were significant differences between BDE-47 exposure groups of 12.5 mg/kg/day, 25 mg/kg/day, 50 mg/kg/day or 100 mg/kg/day and the control group ($P < 0.05$ or $P < 0.01$). Compared with the control group, the ratio of LC3II/LC3I in protein expression levels also decreased significantly in BDE-47 exposure groups ($P < 0.01$). However, the protein expression of P62 increased significantly with the increase of BDE-47 exposure dose, and there were significant differences between 50 mg/kg/day group or 100 mg/kg/day group and the control group ($P < 0.01$).

### 3.5. Mitophagy activating alleviated liver injury induced by BDE-47 in mice

Previous experiments have shown that at an intervention dose of 50 mg/kg/d of BDE-47, mice exhibited significant liver injury, mitochondrial damage, and activation of the NLRP3 inflammasome pathway. Therefore, in this experiment, we continued to select 50 mg/kg/d of BDE-47 as the intervention condition. As demonstrated in the study by

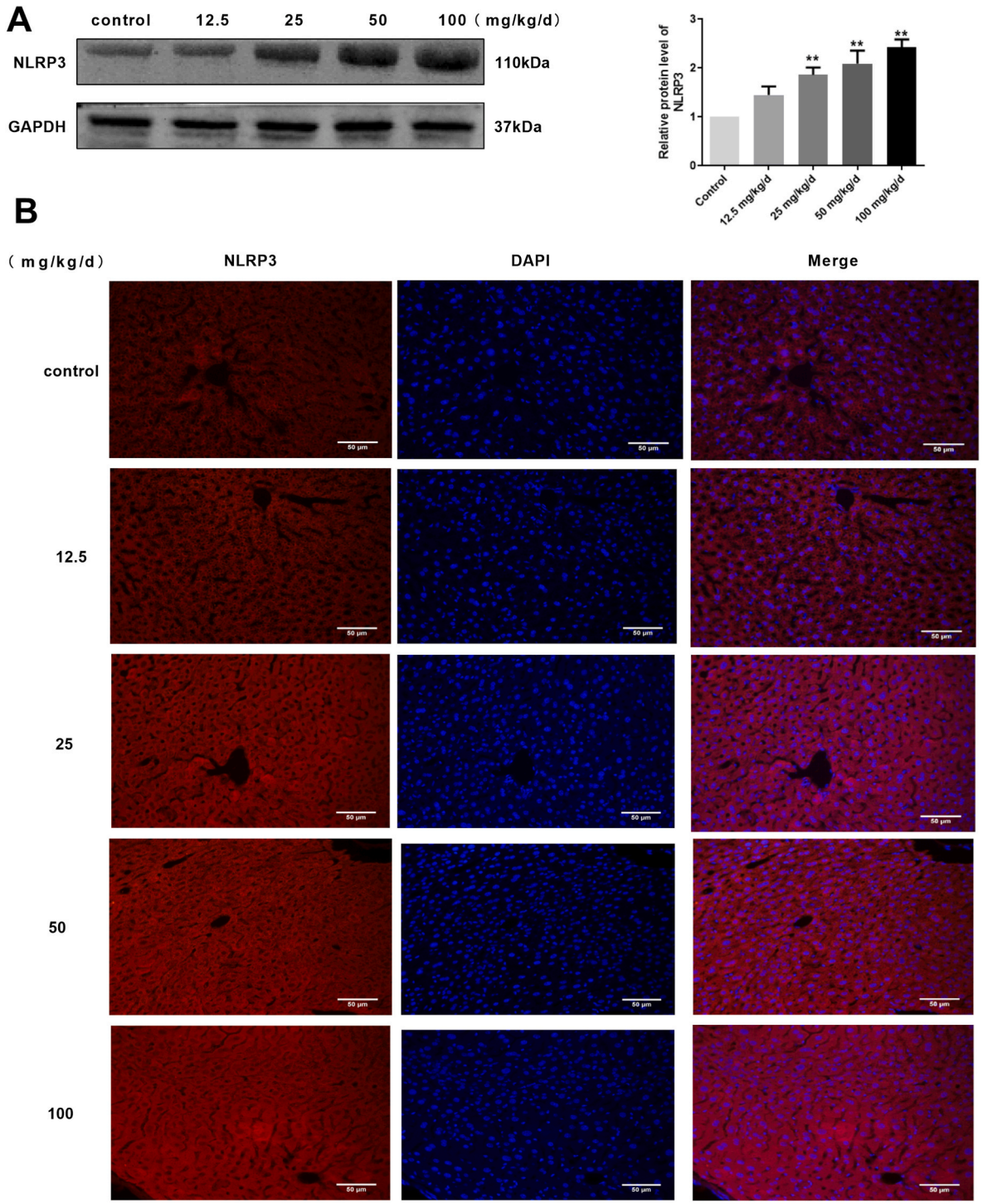


**Fig. 3.** NLRP3 protein expressions in BDE-47 treated mouse liver. A Western Blot assay of mouse liver tissue levels of NLRP3; B Immunofluorescence detection of NLRP3 levels in liver tissues, red fluorescence for NLRP3, blue fluorescence for DAPI (bar = 50 μm). Data are expressed as mean ± SD. n = 4. $^{**}P < 0.01$ compared to control group. BDE-47: 2′,4,4′-tetrabrominated diphenyl ethers. (For interpretation of the references to colour in this figure legend, the reader is referred to the Web version of this article.)

Cho et al., 5 mg/kg/d of RAPA significantly activated mitophagy and alleviated aflatoxin B1-induced liver injury(Cho et al., 2014). Accordingly, this experiment employed 5 mg/kg/d of RAPA to observe its antagonistic effects against BDE-47. The proteins related to mitophagy pathway were determined in the liver in this study. As shown in Fig. 5A, RAPA, an autophagy activator, extremely significantly increased the protein expression of PINK1 and Parkin in liver tissues ($P < 0.01$) and this indicated RAPA activated mitophagy of mice. Subsequently, liver functions were measured and increasing of ALT and AST levels in serum induced by BDE-47 exposure was decreased after treatment of RAPA ($P < 0.05$ or $P < 0.01$), see Fig. 5B. In addition, H&E staining revealed no obvious swelling of hepatocytes and intercellular space increasing in the combined RAPA and BDE-47 exposure group compared with the BDE-47 group (Fig. 5C). Moreover, the decrease of MMP in BDE-47 group was also reversed after adding RAPA, and there was significant increase in the combined RAPA and BDE-47 exposure group as compared with the

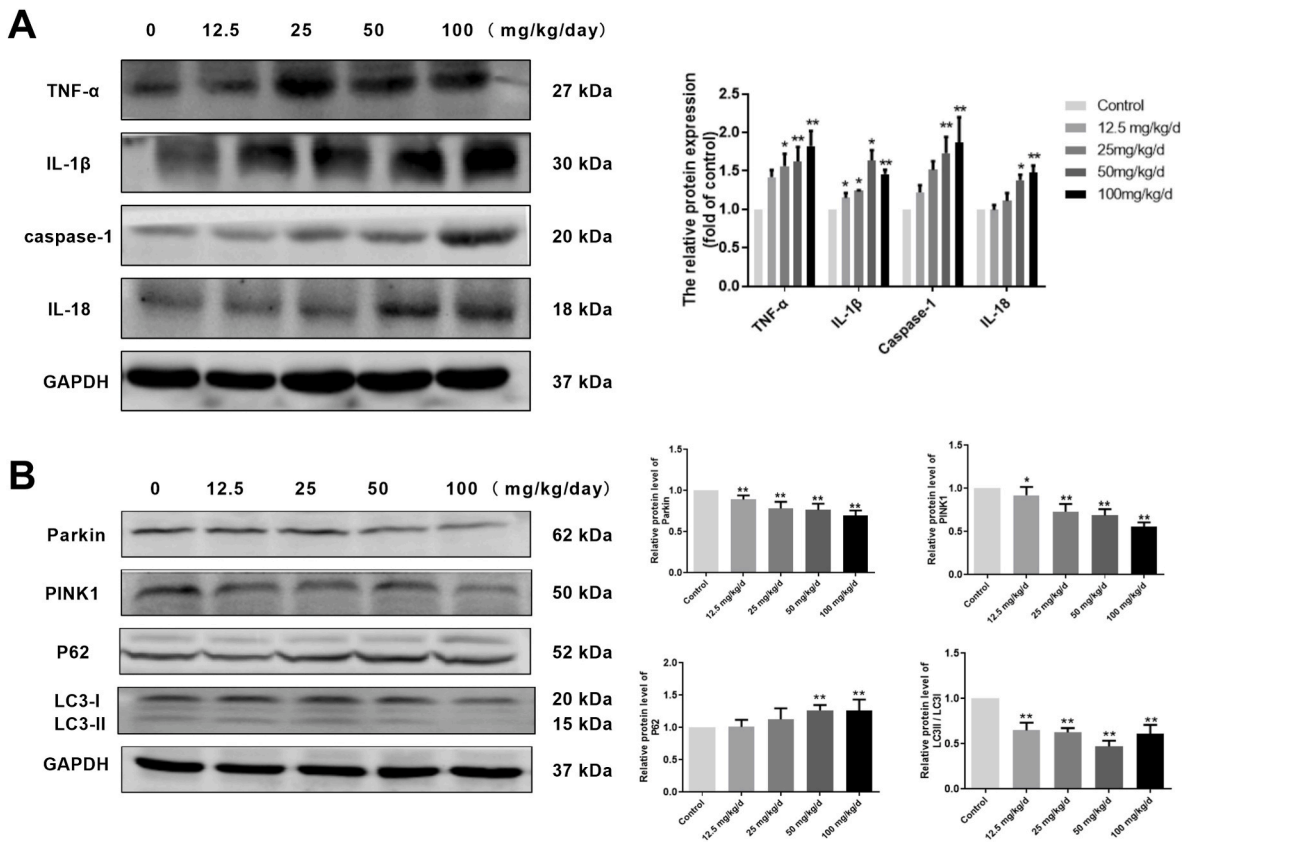


**Fig. 4.** Effects of BDE-47 on mitophagy and inflammatory factors in mouse liver. A The protein levels of TNF-α, IL-1β, Caspase-1, IL-18; B The protein levels of Parkin, PINK1, P62, LC3II, LC3I. Data are expressed as mean ± SD. n = 4. *$P < 0.05$ and **$P < 0.01$ compared to control group. BDE-47: 2′,4,4′-tetrabrominated diphenyl ethers.

BDE-47 group ($P < 0.01$) (Fig. 5D). NLRP3 protein expression significantly increased in the BDE-47 group, whereas RAPA decreased the expression of NLRP3 induced by BDE-47 ($P < 0.05$). Similarly, the protein expression of TNF-α, caspase-1, IL-18 and IL-1β in BDE-47 exposure groups was also reduced by RAPA ($P < 0.05$ or $P < 0.01$), see Fig. 5E.

## 4. Discussion

Exposure to BDE-47 was closely associated with the occurrence of liver disease (Zhang et al., 2024). The liver, as a key organ of drug/xenobiotic metabolism and detoxification, is most vulnerable to external stimuli and damaged. It was reported that continuous exposure to 150 mg/kg/day BDE-47 by Gavage for three months caused significant liver damage in mice, characterized by hepatocyte hypertrophy, vacuolar degeneration, inflammatory cell infiltration and accompanied by increasing of ALT level in serum (Zhang et al., 2015b). ALT and AST are two very commonly used indicators that represents the state of liver function, and ALT and AST could enter the blood and rise abnormally in serum when liver cells are damaged. In this study, we also found the increasing of ALT and AST in serum and histopathological change of liver in BDE-47 exposure mice, which indicated that subacute exposure to BDE-47 led to liver injury. NLRP3 inflammasome, as a pathway of inflammation regulation, plays an important role in various toxicant-mediated liver injury. Exogenous toxins could cause liver damage by activating NLRP3 inflammasome, leading to the release of inflammatory factors downstream of NLRP3. The tetrachloromethane activated the NLRP3 inflammasome in the liver, increasing protein expression of pro-caspase1 and pro-IL-1β, which in turn caused fibrotic damage in liver of mice (Zhang et al., 2020). Arsenic exposure also activated NLRP3 inflammasome in mouse hepatocytes, prompting the release of inflammatory factors of NLRP3 downstream, leading to liver damage in mice (Qiu et al., 2018). However, few studies reported inflammatory injury of liver induced by BDE-47. Chronic exposure to BDE-47 has been reported to result in inflammatory cell infiltration in the pancreas and increased expression of the inflammatory cytokines TNF-α and IL-6 (Qi et al., 2024). BDE-47 increased expressions of NLRP3 and caspase-1, and the levels of IL-1β, IL-6 and TNF-α in mouse organ of Corti-derived cell lines (Tang et al., 2021). In this study, we observed that BDE-47 up-regulated NLRP3 protein levels, and proteins expression of caspase-1, IL-1β, IL-18 and TNF-α inflammatory factors. The immunofluorescence results also indicated that the NLRP3 protein expression in the liver of mice increased after BDE-47 exposure. The results suggested that BDE-47 exposure might cause inflammatory damage by activating the NLRP3 inflammasome in mouse liver.

Mitochondria are the first line of defense against various stress, and affect the pathological process of many diseases. Several studies have demonstrated that mitochondria are the major target subcellular structure of BDE-47. Sun et al. (2021) found that BDE-47 caused dysfunction of pig kidney epithelial cells by inducing mitochondrial abnormalities, leading to ROS increase. BDE-47 affected zebrafish embryonic development by impairing mitochondrial biosynthetic and mitochondrial kinetic (Zhuang et al., 2020). Our results showed that BDE-47 could damage mitochondria, such as obvious swelling, irregular morphology, rupture of mitochondrial membrane, and decrease of MMP, which indicated that BDE-47 exposure could cause mitochondrial injury. When mitochondria are stimulated internally or externally, cells initiate mitophagy to remove and isolate damaged or unwanted mitochondria to maintain cellular homeostasis (Teresak et al., 2022). One of the most classical pathways for mitophagy is the PINK/Parkin pathway. Parkin, as an E3 ubiquitin ligase, could promote autophagosome phagocytosis of mitochondria and shift to depolarized mitochondria, thereby selectively

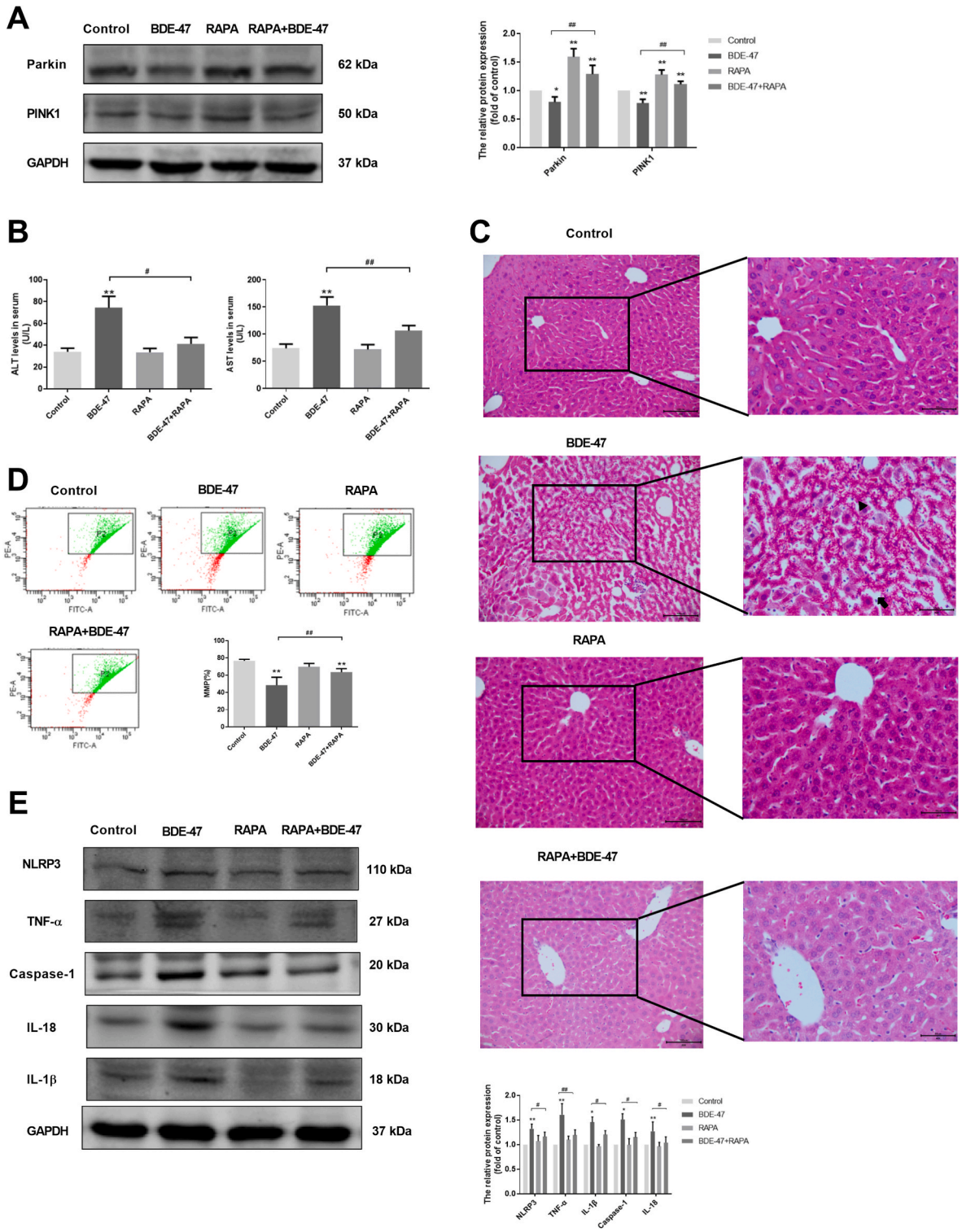


**Fig. 5.** Activation of mitophagy alleviated the liver injury induced by BDE-47 in mice. A Western Blot assay of protein levels of Parkin and PINK1 in liver tissues after with RAPA and/or BDE-47, n = 4; B ALT and AST levels in serum of mice, n = 5; C Representative images of H&E staining. Magnification: 20× and 40 × , Bar = 100 μm and 50 μm. Black triangle: enlarged spaces; Black thick arrowhead: cell swelling; D Flow cytometry detection of MMP in mouse liver, n = 5; E The protein levels of NLRP3, TNF-α, IL-1β, Caspase-1, IL-18, n = 4. Data are expressed as mean ± SD. $^{*}P < 0.05$ and $^{**}P < 0.01$ compared to control group; $\#P < 0.05$ and $\#\#P < 0.01$ compared to BDE-47 group. RAPA: rapamycin, an autophagy activator. BDE-47: 2′,4,4′-tetrabrominated diphenyl ethers. (For interpretation of the references to colour in this figure legend, the reader is referred to the Web version of this article.)

removing damaged mitochondria (Ma et al., 2020). Then, Parkin was recruited to damaged mitochondria by PINK1 to initiate mitophagy. Accumulating evidence indicated that external chemicals might active mitophagy, such as, aflatoxins B1 activated PINK1/Parkin-mediated mitophagy in mouse hepatocytes (Wang et al., 2022), cadmium induced mitophagy in PC12 cells dependent on the PINK1/Parkin pathway (Wang et al., 2020), and manganese could induce mitophagy in SH-SY5Y cells by increasing proteins of PINK1, Parkin and LC3 (Zhang

et al., 2016). However, BDE-47 had been shown to cause mitochondrial dysfunction and associated oxidative liver damage by impairing mitophagy (Chen et al., 2020). Our results were consistent with the study and showed that the protein expression of PINK1/Parkin pathway and LC3 protein decreased with the increase of BDE-47 exposure dose. PINK1/Parkin-mediated mitophagy play a protective role by selective removal of damaged mitochondria. We speculated that BDE-47 might inhibit mitophagy and lead to increase of damaged mitochondria in the hepatocytes and further exacerbating the damage of liver. Autophagy adaptor protein p62, as a downstream functional protein of ubiquitination, can promote mitochondrial ubiquitination. Mitochondrial ubiquitination promoted by P62 led to degradation of outer membrane proteins and aggravated mitochondrial damage, resulted in liver injury (Mai et al., 2019). We found that p62 protein increased with the increase of BDE-47 exposure dose, which indicated that p62 might be involved in liver injury in BDE-47 exposure mice.

As an energy source for eukaryotes, mitochondria generates ROS during electron transport in the respiratory chain and balances redox processes through mitophagy. In this study, the increase of ROS in BDE-47 exposure group might be mitophagy reducing, which resulted in a decrease to clear damaged mitochondria. In an acute kidney injury model, mitophagy mediated through PINK1/Parkin prevented tubular epithelial cell apoptosis and kidney damage by decreasing mitochondrial ROS and NLRP3 inflammasome activation (Lin et al., 2019). It is noteworthy that the role of ROS in autophagy regulation is dual. While moderate ROS levels have been shown to activate autophagy as an adaptive response, excessive and sustained ROS generation (Ornatowski et al., 2020). As induced by high-dose BDE-47 in this study, can disrupt mitochondrial function and impair the autophagy machinery. In our model, the observed suppression of PINK1/Parkin-mediated mitophagy, coupled with significant ROS elevation, suggests that the oxidative stress exceeded the threshold beyond which autophagy remains protective. This imbalance likely contributed to the accumulation of damaged mitochondria and subsequent NLRP3 inflammasome activation. Palmatine can protect mice from dextran sulfate sodium-induced colitis by promoting PINK1/Parkin-driven mitophagy to clear damaged mitochondria, inhibiting NLRP3 inflammasome activation in macrophages (Mai et al., 2019). Resveratrol might inhibit the activation of NLRP3 inflammasomes by promoting PINK1/Parkin-mediated mitophagy, which reduced mitochondrial membrane potential levels, and alleviated mitochondrial damage in arthritis rat models (Fan et al., 2021). By removing the NLRP3 inflammasome activator, mitophagy reduce inflammasome activation and inflammatory response. The autophagy dysfunction led to diseases associated with excessive inflammation and over-activation of NLRP3 inflammasomes (Biasizzo and Kopitar-Jerala, 2020). Previous studies have reported that mitochondrial ROS and metabolic stress are associated with mTOR inhibition or activation (Dodson et al., 2013). Therefore, inhibiting mTOR pathway activity contributes to the promotion of mitophagy. RAPA is a macrocyclic triene antibiotic that binds to and inhibits the molecular target of mTOR. In this study, RAPA, an autophagy activator, increased mitophagy activity, inhibited the activation of NLRP3 inflammasome and the release of inflammatory factors, and attenuated BDE-47-induced mitochondrial damage and liver injury. Collectively, our results and these research reports revealed the role of mitophagy in removing defective mitochondria by modulating NLRP3 inflammasome.

However, although BDE-47 exposure increased NLRP3 inflammasome and the expression of downstream inflammatory factors, the role of NLRP3 inflammasome and inflammatory factors in liver injury of mice has not been verified by application of NLRP3 inhibitor or siRNA targeting NLRP3.

## 5. Conclusion

Our current research presented the damage of mitochondrial and liver mediated by NLRP3 inflammasome activation via mitophagy downregulation in BDE-47-exposed mice. Mitophagy activating can alleviate inflammatory damage in mouse liver by regulating NLRP3 inflammasome.

## CRediT authorship contribution statement

**Xiyue Cao:** Writing – original draft, Conceptualization. **Weijue Liu:** Formal analysis, Data curation. **Shuhua Xi:** Writing – review & editing, Funding acquisition. **Yue Wang:** Writing – review & editing, Writing – original draft.

## Funding

This work was supported by the National Key Research and Development Program of China (Grant No. 2018YFC1801204).

## Declaration of competing interest

The authors declare that they have no known competing financial interests or personal relationships that could have appeared to influence the work reported in this paper.

## Appendix A. Supplementary data

Supplementary data to this article can be found online at https://doi.org/10.1016/j.fct.2025.115738.

## Data availability

Data will be made available on request.

## References

Biasizzo, M., Kopitar-Jerala, N., 2020. Interplay between NLRP3 inflammasome and autophagy. Front. Immunol. 11, 591803. https://doi.org/10.3389/fimmu.2020.591803.

Chen, F., Feng, L., Zheng, Y.L., et al., 2020. 2, 2', 4, 4'-tetrabromodiphenyl ether (BDE-47) induces mitochondrial dysfunction and related liver injury via eliciting miR-34a-5p-mediated mitophagy impairment. Environ. Pollut. 258, 113693. https://doi.org/10.1016/j.envpol.2019.113693.

Cho, H.I., Choi, J.W., Lee, S.M., 2014. Impairment of autophagosome-lysosome fusion contributes to chronic ethanol-induced liver injury. Alcohol 48, 717–725. https://doi.org/10.1016/j.alcohol.2014.08.006.

Doblado, L., Lueck, C., Rey, C., et al., 2021. Mitophagy in human diseases. Int. J. Mol. Sci. 22, 3903. https://doi.org/10.3390/ijms22083903.

Dodson, M., Darley-Usmar, V., Zhang, J., 2013. Cellular metabolic and autophagic pathways: traffic control by redox signaling. Free Radic. Biol. Med. 63, 207–221. https://doi.org/10.1016/j.freeradbiomed.2013.05.014.

Dong, L., Sun, Q., Qiu, H., et al., 2023. Melatonin protects against developmental PBDE-47 neurotoxicity by targeting the AMPK/mitophagy axis. J. Pineal Res. 75, e12871. https://doi.org/10.1111/jpi.12871.

Fan, W., Chen, S., Wu, X., et al., 2021. Resveratrol relieves gouty arthritis by promoting mitophagy to inhibit activation of NLRP3 inflammasomes. J. Inflamm. Res. 14, 3523–3536. https://doi.org/10.2147/JIR.S320912.

Foster, W.G., Gregorovich, S., Morrison, K.M., Atkinson, S.A., Kubwabo, C., Stewart, B., Teo, K., 2011. Human maternal and umbilical cord blood concentrations of polybrominated diphenyl ethers. Chemosphere 84, 1301–1309. https://doi.org/10.1016/j.chemosphere.2011.05.028.

Fromme, H., Becher, G., Hilger, B., Völkel, W., 2016. Brominated flame retardants - exposure and risk assessment for the general population. Int. J. Hyg Environ. Health 219, 1–23. https://doi.org/10.1016/j.ijheh.2015.08.004.

Gomez, M.V., Dutta, M., Suvorov, A., et al., 2015. Toxicity of brominated flame retardants, BDE-47 and BDE-99 stems from impaired mitochondrial bioenergetics. Toxicol. Mech. Methods 25, 34–41. https://doi.org/10.3109/15376516.2014.974233.

Han, H., Tan, J., Wang, R., et al., 2020. PINK1 phosphorylates Drp1$^{S616}$ to regulate mitophagy-independent mitochondrial dynamics. EMBO Rep. 21, e48686. https://doi.org/10.15252/embr.201948686.

Hu, J., Jin, J., Wang, Y., Ma, Z., Zheng, W., 2011. Levels of polybrominated diphenyl ethers and hexabromocyclododecane in the atmosphere and tree bark from beijing, China. Chemosphere 84, 355–360. https://doi.org/10.1016/j.chemosphere.

Kelley, N., Jeltema, D., Duan, Y., et al., 2019. The NLRP3 inflammasome: an overview of mechanisms of activation and regulation. Int. J. Mol. Sci. 20, 3328. https://doi.org/10.3390/ijms20133328.

Lin, Q., Li, S., Jiang, N., et al., 2019. PINK1-parkin pathway of mitophagy protects against contrast-induced acute kidney injury via decreasing mitochondrial ROS and

NLRP3 inflammasome activation. Redox Biol. 26, 101254. https://doi.org/10.1016/j.redox.2019.101254.
Liu, W., Li, S., Zhou, Q., et al., 2022. 2, 2', 4, 4'-tetrabromodiphenyl ether induces placental toxicity via activation of p38 MAPK signaling pathway in vivo and in vitro. Ecotoxicol. Environ. Saf. 244, 114034. https://doi.org/10.1016/j.ecoenv.2022.114034.
Ma, X., McKeen, T., Zhang, J., et al., 2020. Role and mechanisms of mitophagy in liver diseases. Cells 9, 837. https://doi.org/10.3390/cells9040837.
Mai, C.T., Wu, M.M., Wang, C.L., et al., 2019. Palmatine attenuated dextran sulfate sodium (DSS)-Induced colitis via promoting mitophagy-mediated NLRP3 inflammasome inactivation. Mol. Immunol. 105, 76–85. https://doi.org/10.1016/j.molimm.2018.10.015.
Meng, S., Chen, X., Gyimah, E., et al., 2020. Hepatic oxidative stress, DNA damage and apoptosis in adult zebrafish following sub-chronic exposure to BDE-47 and BDE-153. Environ. Toxicol. 35, 1202–1211. https://doi.org/10.1002/tox.22985.
Ornatowski, W., Lu, Q., Yegambaram, M., Garcia, A.E., Zemskov, E.A., Maltepe, E., Fineman, J.R., Wang, T., Black, S.M., 2020. Complex interplay between autophagy and oxidative stress in the development of pulmonary disease. Redox Biol. 36, 101679. https://doi.org/10.1016/j.redox.2020.101679.
Pickrell, A.M., Youle, R.J., 2015. The roles of PINK1, parkin, and mitochondrial fidelity in parkinson's disease. Neuron 85, 257–273. https://doi.org/10.1016/j.neuron.2014.12.007.
Qi, X., Liu, Q., Wei, Z., et al., 2024. Chronic exposure to BDE-47 aggravates acute pancreatitis and chronic pancreatitis by promoting acinar cell apoptosis and inflammation. Toxicol. Sci. 199, 120–131. https://doi.org/10.1093/toxsci/kfae024.
Qiu, T., Pei, P., Yao, X., et al., 2018. Taurine attenuates arsenic-induced pyroptosis and nonalcoholic steatohepatitis by inhibiting the autophagic-inflammasomal pathway. Cell Death Dis. 9, 946. https://doi.org/10.1038/s41419-018-1004-0.
Shan, S., Shen, Z., Zhang, C., et al., 2019. Mitophagy protects against acetaminophen-induced acute liver injury in mice through inhibiting NLRP3 inflammasome activation. Biochem. Pharmacol. 169, 113643. https://doi.org/10.1016/j.bcp.2019.113643.
Sun, S., Zhao, Z., Rao, Q., et al., 2021. BDE-47 induces nephrotoxicity through ROS-dependent pathways of mitochondrial dynamics in PK15 cells. Ecotoxicol. Environ. Saf. 222, 112549. https://doi.org/10.1016/j.ecoenv.2021.112549.
Tang, J., Hu, B., Zheng, H., et al., 2021. 2,2',4,4'-Tetrabromodiphenyl ether (BDE-47) activates aryl hydrocarbon receptor (AhR) mediated ROS and NLRP3 inflammasome/p38 MAPK pathway inducing necrosis in cochlear hair cells. Ecotoxicol. Environ. Saf. 221, 112423. https://doi.org/10.1016/j.ecoenv.2021.112423.
Teresak, P., Lapao, A., Subic, N., et al., 2022. Regulation of PRKN independent mitophagy. Autophagy 18, 24–39. https://doi.org/10.1080/15548627.2021.1888244.
Wang, Q., Jia, F., Guo, C., et al., 2022. PINK1/Parkinmediated mitophagy as a protective mechanism against AFB(1)-induced liver injury in mice. Food Chem. Toxicol. 164, 113043. https://doi.org/10.1016/j.fct.2022.113043.
Wang, T., Zhu, Q., Cao, B., et al., 2020. Cadmium induces mitophagy via AMP activated protein kinases activation in a PINK1/Parkin-dependent manner in PC12 cells. Cell Prolif. 53, e12817. https://doi.org/10.1111/cpr.12817.
Zhang, H.T., Mi, L., Wang, T., et al., 2016. PINK1/Parkin-mediated mitophagy play a protective role in manganese induced apoptosis in SH-SY5Y cells. Toxicol. Vitro 34, 212–219. https://doi.org/10.1016/j.tiv.2016.04.006.
Zhang, X., Huang, Y., Yang, L., et al., 2024. Dietary exposure to 2,2',4,4'-tetrabromodiphenyl ether (BDE-47) induces oxidative damage promoting cell apoptosis primarily via mitochondrial pathway in the hepatopancreas of carp, Cyprinus carpio. Ecotoxicol. Environ. Saf. 274, 116192. https://doi.org/10.1016/j.ecoenv.2024.116192.
Zhang, X., Kuang, G., Wan, J., et al., 2020. Salidroside protects mice against CCl4-induced acute liver injury via down-regulating CYP2E1 expression and inhibiting NLRP3 inflammasome activation. Int. Immunopharmacol. 85, 106662. https://doi.org/10.1016/j.intimp.2020.106662.
Zhang, Y., Hu, B., Qian, X., et al., 2022. Transcriptomics-based analysis of co-exposure of cadmium (Cd) and 2,2',4,4'-tetrabromodiphenyl ether (BDE-47) indicates mitochondrial dysfunction induces NLRP3 inflammasome and inflammatory cell death in renal tubular epithelial cells. Ecotoxicol. Environ. Saf. 241, 113790. https://doi.org/10.1016/j.ecoenv.2022.113790.
Zhang, Z.F., Shan, Q., Zhuang, J., et al., 2015a. Troxerutin inhibits 2,2',4,4'-tetrabromodiphenyl ether (BDE-47)-induced hepatocyte apoptosis by restoring proteasome function. Toxicol. Lett. 233, 246–257. https://doi.org/10.1016/j.toxlet.2015.01.017.
Zhang, Z.F., Zhang, Y.Q., Fan, S.H., et al., 2015b. Troxerutin protects against 2,2',4,4'-tetrabromodiphenyl ether (BDE-47)-induced liver inflammation by attenuating oxidative stress-mediated $NAD^+$-depletion. J. Hazard Mater. 283, 98–109. https://doi.org/10.1016/j.jhazmat.2014.09.012.
Zhuang, J., Pan, Z.J., Li, M., et al., 2020. BDE-47 induced apoptosis in zebrafish embryos through mitochondrial ROS-mediated JNK signaling. Chemosphere 258, 127385. https://doi.org/10.1016/j.chemosphere.2020.127385.